

Chapter 1. Flow around a cylinder in steady current

1.1 Regimes of flow around a smooth, circular cylinder

The non-dimensional quantities describing the flow around a smooth circular cylinder depend on the cylinder Reynolds number

$$Re = \frac{DU}{\nu} \tag{1.1}$$

in which D is the diameter of the cylinder, U is the flow velocity, and ν is the kinematic viscosity. The flow undergoes tremendous changes as the Reynolds number is increased from zero. The flow regimes experienced with increasing Re are summarized in Fig. 1.1. Fig. 1.2, on the other hand, gives the definition sketch regarding the two different flow regions referred to in Fig. 1.1, namely the wake and the boundary layer. While the wake extends over a distance which is comparable with the cylinder diameter, D , the boundary layer extends over a very small thickness, δ , which is normally small compared with D . The boundary layer thickness, in the case of laminar boundary layer, for example, is (Schlichting, 1979)


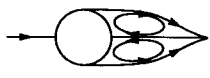


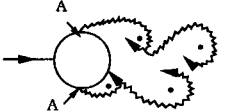
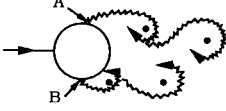
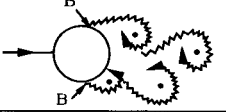
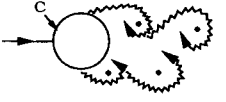
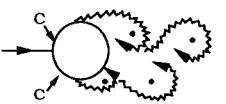
<p>a)</p> 	<p>No separation. Creeping flow</p>	<p>$Re < 5$</p>
<p>b)</p> 	<p>A fixed pair of symmetric vortices</p>	<p>$5 < Re < 40$</p>
<p>c)</p> 	<p>Laminar vortex street</p>	<p>$40 < Re < 200$</p>
<p>d)</p> 	<p>Transition to turbulence in the wake</p>	<p>$200 < Re < 300$</p>
<p>e)</p> 	<p>Wake completely turbulent. A: Laminar boundary layer separation</p>	<p>$300 < Re < 3 \times 10^5$ Subcritical</p>
<p>f)</p> 	<p>A: Laminar boundary layer separation B: Turbulent boundary layer separation; but boundary layer laminar</p>	<p>$3 \times 10^5 < Re < 3.5 \times 10^5$ Critical (Lower transition)</p>
<p>g)</p> 	<p>B: Turbulent boundary layer separation; the boundary layer partly laminar partly turbulent</p>	<p>$3.5 \times 10^5 < Re < 1.5 \times 10^6$ Supercritical</p>
<p>h)</p> 	<p>C: Boundary layer com- pletely turbulent at one side</p>	<p>$1.5 \times 10^6 < Re < 4 \times 10^6$ Upper transition</p>
<p>i)</p> 	<p>C: Boundary layer com- pletely turbulent at two sides</p>	<p>$4 \times 10^6 < Re$ Transcritical</p>

Figure 1.1 Regimes of flow around a smooth, circular cylinder in steady current.

$$\frac{\delta}{D} = O\left(\frac{1}{\sqrt{Re}}\right) \quad (1.2)$$

and it is seen that $\delta/D \ll 1$ for Re larger than $O(100)$, say.

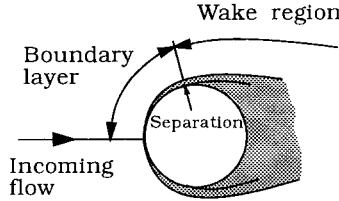


Figure 1.2 Definition sketch.

Now, returning to Fig. 1.1, for very small values of Re no separation occurs. The separation first appears when Re becomes 5 (Figs. 1.1a).

For the range of the Reynolds number $5 < Re < 40$, a fixed pair of vortices forms in the wake of the cylinder (Fig. 1.1 b). The length of this vortex formation increases with Re (Batchelor, 1967).

When the Reynolds number is further increased, the wake becomes unstable, which would eventually give birth to the phenomenon called vortex shedding in which vortices are shed alternately at either side of the cylinder at a certain frequency. Consequently, the wake has an appearance of a vortex street (see Fig. 1.3d-f).

For the range of the Reynolds number $40 < Re < 200$ the vortex street is laminar (Fig. 1.1c). The shedding is essentially two-dimensional, i.e., it does not vary in the spanwise direction (Williamson, 1989).

With a further increase in Re , however, transition to turbulence occurs in the wake region (Fig. 1.1d). The region of transition to turbulence moves towards the cylinder, as Re is increased in the range $200 < Re < 300$ (Bloor, 1964). Bloor (1964) reports that at $Re = 400$, the vortices, once formed, are turbulent. Observations show that the two-dimensional feature of the vortex shedding observed in the range $40 < Re < 200$ becomes distinctly three-dimensional in this range (Gerard, 1978 and Williamson, 1988); the vortices are shed in cells in the spanwise direction. (It may be noted that this feature of vortex shedding prevails for all the other Reynolds number regimes $Re > 300$. This topic will be studied in some detail in Section 1.2.2 in the context of correlation length).

For $Re > 300$, the wake is completely turbulent. The boundary layer over the cylinder surface remains laminar, however, for increasing Re over a very wide

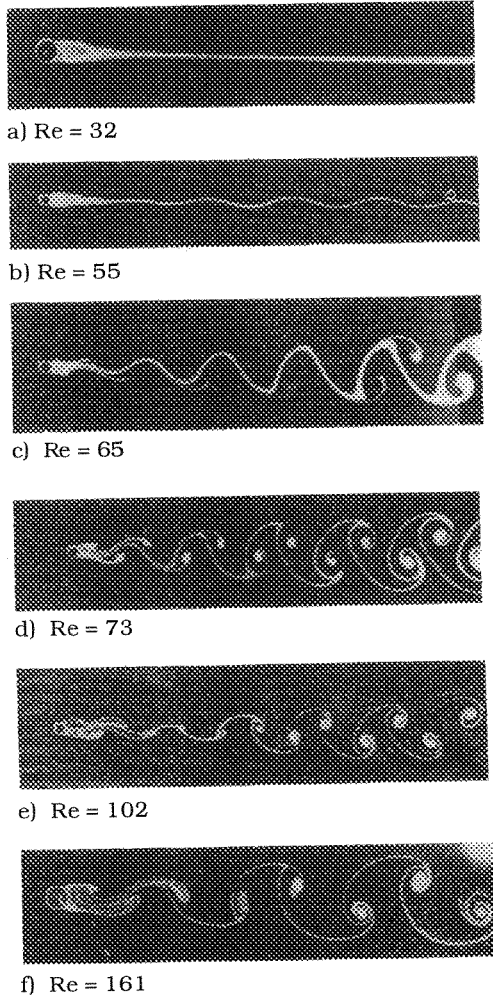


Figure 1.3 Appearance of vortex shedding behind a circular cylinder in a stream of oil (from Homann, 1936) with increasing Re .

range of Re , namely $300 < Re < 3 \times 10^5$. This regime is known as the subcritical flow regime (Fig. 1.1e).

With a further increase in Re , transition to turbulence occurs in the boundary layer itself. The transition first takes place at the point where the boundary layer separates, and then the region of transition to turbulence moves upstream over the cylinder surface towards the stagnation point as Re is increased (Figs. 1.1f – 1.1i).

In the narrow Re band $3 \times 10^5 < Re < 3.5 \times 10^5$ (Fig. 1.1f) the boundary layer becomes turbulent at the separation point, but this occurs only at one side of the cylinder. So the boundary layer separation is turbulent on one side of the cylinder and laminar on the other side. This flow regime is called the critical (or the lower transition) flow regime. The flow asymmetry causes a non-zero mean lift on the cylinder, as seen from Fig. 1.4.

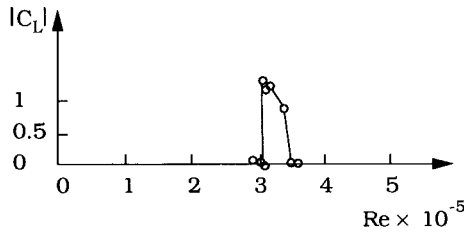


Figure 1.4 Non-zero mean lift in the critical-flow regime ($3 \times 10^5 < Re < 3.5 \times 10^5$). Schewe (1983).

The side at which the separation is turbulent switches from one side to the other occasionally (Schewe, 1983). Therefore, the lift changes direction, as the one-sided transition to turbulence changes side, shifting from one side to the other (Schewe, 1983).

The next Reynolds number regime is the so-called supercritical flow regime where $3.5 \times 10^5 < Re < 1.5 \times 10^6$ (Fig. 1.1g). In this regime, the boundary layer separation is turbulent on both sides of the cylinder. However, transition to turbulence in the boundary layer has not been completed yet; the region of transition to turbulence is located somewhere between the stagnation point and the separation point.

The boundary layer on one side becomes fully turbulent when Re reaches the value of about 1.5×10^6 . So, in this flow regime, the boundary layer is completely turbulent on one side of the cylinder and partly laminar and partly turbulent on

the other side. This type of flow regime, called the upper-transition flow regime, prevails over the range of Re , $1.5 \times 10^6 < Re < 4.5 \times 10^6$ (Fig. 1.1h).

Finally, when Re is increased so that $Re > 4.5 \times 10^6$, the boundary layer over the cylinder surface is virtually turbulent everywhere. This flow regime is called the transcritical flow regime.

Regarding the terminology in relation to the described flow regimes and also the ranges of Re in which they occur, there seems to be no general consensus among various authors (Farell, 1981). The preceding classification and the description are mainly based on Roshko's (1961) and Schewe's (1983) works. Roshko's work covered the Reynolds number range from 10^6 to 10^7 , which revealed the existence of the upper transition and the transcritical regimes, while Schewe's work, covering the range $2.3 \times 10^4 < Re < 7.1 \times 10^6$, clarified further details of the flow regimes from the lower transition to the transcritical flow regimes.

1.2 Vortex shedding

The most important feature of the flow regimes described in the previous section is the vortex-shedding phenomenon, which is common to all the flow regimes for $Re > 40$ (Fig. 1.1). For these values of Re , the boundary layer over the cylinder surface will separate due to the adverse pressure gradient imposed by the divergent geometry of the flow environment at the rear side of the cylinder. As a result of this, a shear layer is formed, as sketched in Fig. 1.5.

As seen from Fig. 1.6, the boundary layer formed along the cylinder contains a significant amount of vorticity. This vorticity is fed into the shear layer formed downstream of the separation point and causes the shear layer to roll up into a vortex with a sign identical to that of the incoming vorticity. (Vortex A in Fig. 1.5).

Likewise, a vortex, rotating in the opposite direction, is formed at the other side of the cylinder (Vortex B).

Mechanism of vortex shedding

It has been mentioned in the previous section that the pair formed by these two vortices is actually unstable when exposed to the small disturbances for Reynolds numbers $Re > 40$. Consequently, one vortex will grow larger than the other if $Re > 40$. Further development of the events leading to vortex shedding has been described by Gerrard (1966) in the following way.

The larger vortex (Vortex A in Fig. 1.7a) presumably becomes strong enough to draw the opposing vortex (Vortex B) across the wake, as sketched in Fig. 1.7a. The vorticity in Vortex A is in the clockwise direction (Fig. 1.5b), while that in Vortex B is in the anti-clockwise direction. The approach of vorticity of

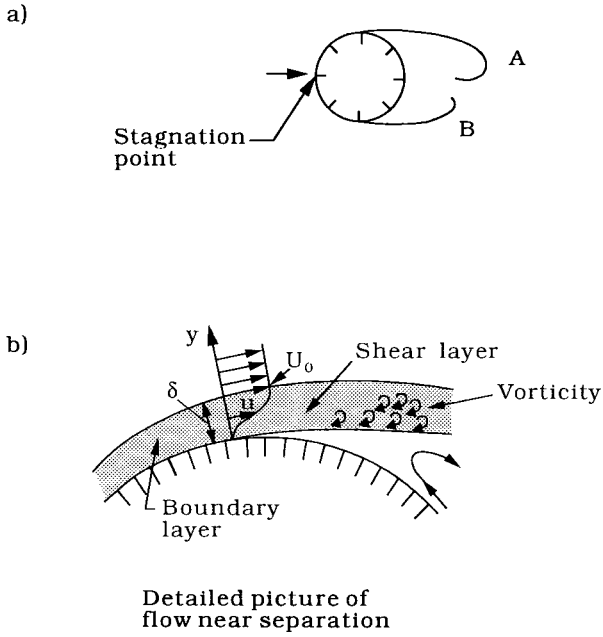


Figure 1.5 The shear layer. The shear layers on both sides roll up to form the lee-wake vortices, Vortices A and B.

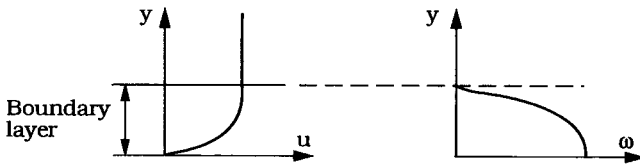


Figure 1.6 Distribution of velocity and vorticity in the boundary layer. ω is the vorticity, namely $\omega = \frac{1}{2} \frac{\partial u}{\partial y}$.

the opposite sign will then cut off further supply of vorticity to Vortex A from its boundary layer. This is the instant where Vortex A is shed. Being a free vortex, Vortex A is then convected downstream by the flow.

Following the shedding of Vortex A, a new vortex will be formed at the same side of the cylinder, namely Vortex C (Fig. 1.7b). Vortex B will now play the same role as Vortex A, namely it will grow in size and strength so that it will draw Vortex C across the wake (Fig. 1.7b). This will lead to the shedding of Vortex B. This process will continue each time a new vortex is shed at one side of the cylinder where the shedding will continue to occur in an alternate manner between the sides of the cylinder.

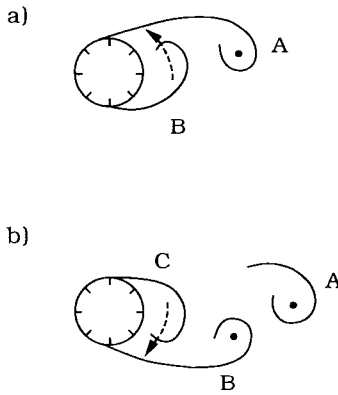


Figure 1.7 (a): Prior to shedding of Vortex A, Vortex B is being drawn across the wake. (b): Prior to shedding of Vortex B, Vortex C is being drawn across the wake.

The sequence of photographs given in Fig. 1.8 illustrates the time development of the process during the course of shedding process.

One implication of the foregoing discussion is that the vortex shedding occurs only when the two shear layers interact with each other. If this interaction is inhibited in one way or another, for example by putting a splitter plate at the downstream side of the cylinder between the two shear layers, the shedding would be prevented, and therefore no vortex shedding would occur in this case. Also, as another example, if the cylinder is placed close to a wall, the wall-side shear layer will not develop as strongly as the opposing shear layer; this will presumably lead to a weak interaction between the shear layers, or to practically no interaction if the cylinder is placed very close to the wall. In such situations, the vortex shed-

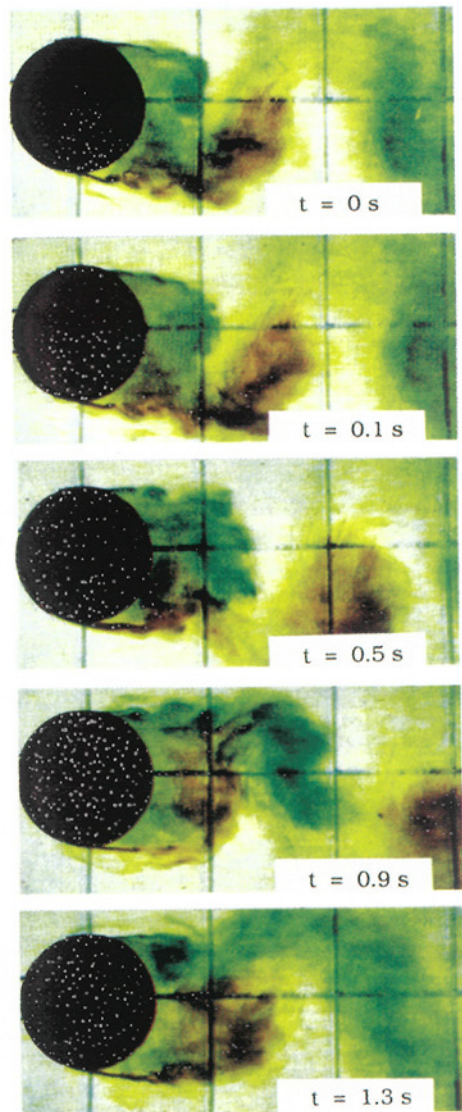


Figure 1.8 Time development of vortex shedding during approximately two-third of the shedding period. $Re = 7 \times 10^3$.

ding is suppressed. The effect of close proximity of a wall on the vortex shedding will be examined in some detail later in the next section.

1.2.1 Vortex-shedding frequency

The vortex-shedding frequency, when normalized with the flow velocity U and the cylinder diameter D , can on dimensional grounds be seen to be a function of the Reynolds number:

$$St = St(Re) \tag{1.3}$$

in which

$$St = \frac{f_v D}{U} \tag{1.4}$$

and f_v is the vortex-shedding frequency. The normalized vortex-shedding frequency, namely St , is called the Strouhal number. Fig. 1.9 illustrates how the Strouhal number varies with Re , while Fig. 1.10 gives the power spectra corresponding to Schewe's (1983) data shown in Fig. 1.9.

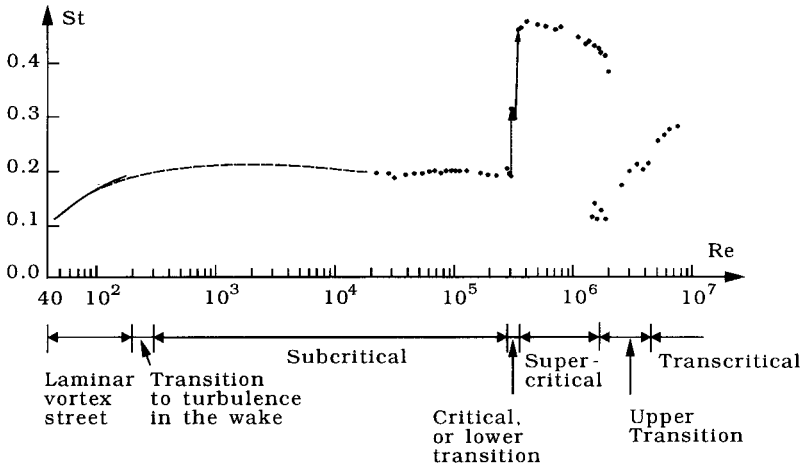


Figure 1.9 Strouhal number for a smooth circular cylinder. Experimental data from: Solid curve: Williamson (1989). Dashed curve: Roshko (1961). Dots: Schewe (1983).

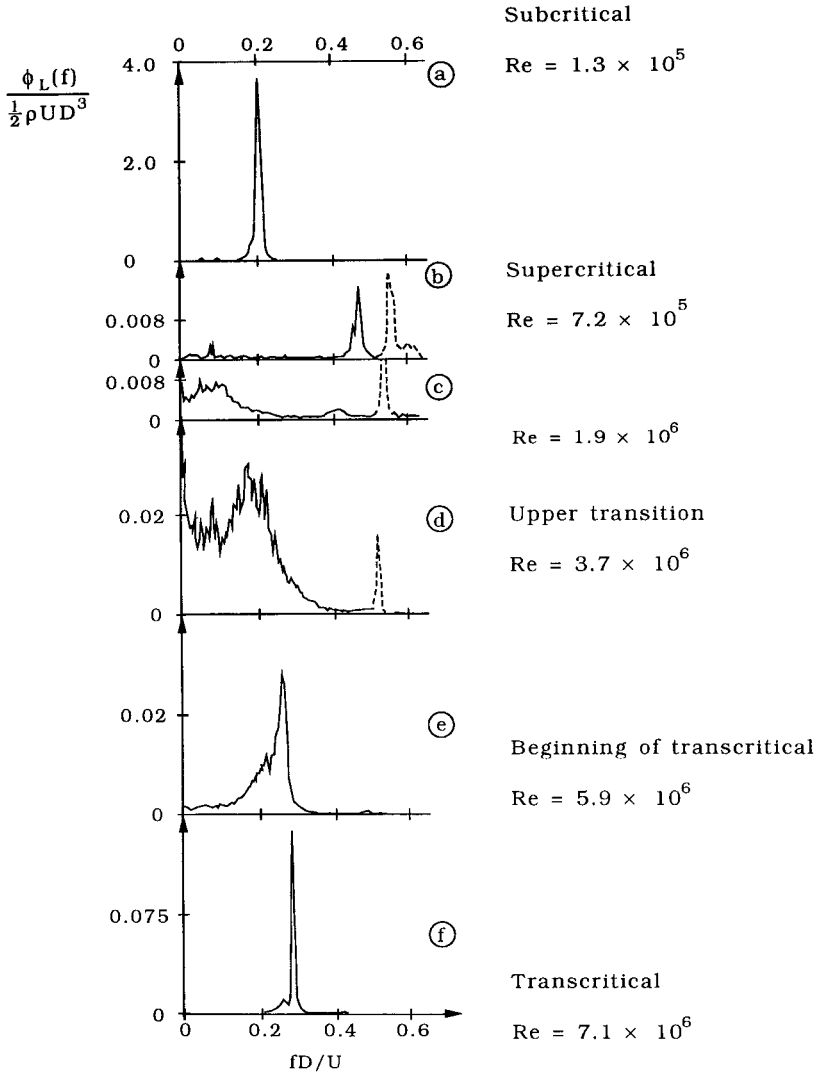


Figure 1.10 Power spectra of the lift oscillations corresponding to Schewe's data in Fig. 1.9 (Schewe, 1983).

The vortex shedding first appears at $Re = 40$. From Fig. 1.9, the shedding frequency St is approximately 0.1 at this Re . It then gradually increases as Re is increased and attains a value of about 0.2 at $Re \cong 300$, the lower end of the subcritical flow regime. From this Re number onwards throughout the subcritical range St remains practically constant (namely, at the value of 0.2).

The narrow-band spectrum with the sharply defined dominant frequency in Fig. 1.10a indicates that vortex shedding in the subcritical range occurs in a well-defined, regular fashion.

As seen from Fig. 1.9, the Strouhal frequency experiences a sudden jump at $Re = 3 - 3.5 \times 10^5$, namely in the critical Re number range, where St increases from 0.2 to a value of about 0.45. This high value of St is maintained over a rather large part of the supercritical Re range, subsequently it decreases slightly with increasing Reynolds number.

The large increase in St in the supercritical-flow range is explained as follows: in the supercritical flow regime, the boundary layer on both sides of the cylinder is turbulent at the separation points. This results in a delay in the boundary-layer separation where the separation points move downstream, as sketched in Fig. 1.11. This means that the vortices (now being closer to each other) would interact at a faster rate than in the subcritical flow regime, which would obviously lead to higher values of the Strouhal number.

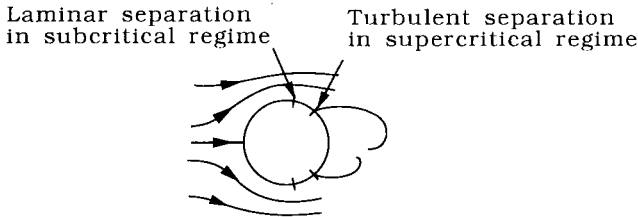


Figure 1.11 Sketch showing positions of separation points at different separation regimes.

The power spectrum (Fig. 1.10b) at $Re = 7.2 \times 10^5$, a Reynolds number which is representative for the supercritical range, indicates that in this Re range, too, the shedding occurs in a well-defined, orderly fashion, since the power spectrum appears to be a narrow-band spectrum with a sharply defined, dominant peak. The fact that the magnitude of the spectrum itself is extremely small (cf. Figs. 1.10a and 1.10b) indicates, however, that the shed vortices are not as strong as they are in the subcritical flow regime. An immediate consequence of this, as will be shown later, is that the lift force induced by the vortex shedding is relatively weak in this Re range.

The Strouhal number experiences yet another discontinuity when Re reaches the value of about 1.5×10^6 . At this Reynolds number, transition to turbulence in one of the boundary layers has been completed (Fig. 1.1h). So, the boundary layer at one side of the cylinder is completely turbulent and that at the other side of the cylinder is partly laminar and partly turbulent, an asymmetric situation with regard to the formation of the lee-wake vortices. This situation prevails over the whole upper transition region (Fig. 1.1h). Now, the asymmetry in the formation of the lee-wake vortices inhibits the interaction of these vortices partially, resulting in an irregular, disorderly vortex shedding. This can be seen clearly from the broad-band spectra in Figs. 1.10c and d.

The regular vortex shedding is re-established, however, (see the narrow-band power spectra in Fig. 1.10e and f), when Re is increased to values larger than approximately 4.5×10^6 , namely the transcritical flow regime where the Strouhal number takes the value of $0.25 - 0.30$ (Fig. 1.9).

Effect of surface roughness

For rough cylinders the normalized shedding frequency, namely the Strouhal number, should be a function of both Re and the relative roughness

$$St = St(Re, k_s/D) \quad (1.5)$$

in which k_s is the Nikuradse's equivalent sand roughness of the cylinder surface.

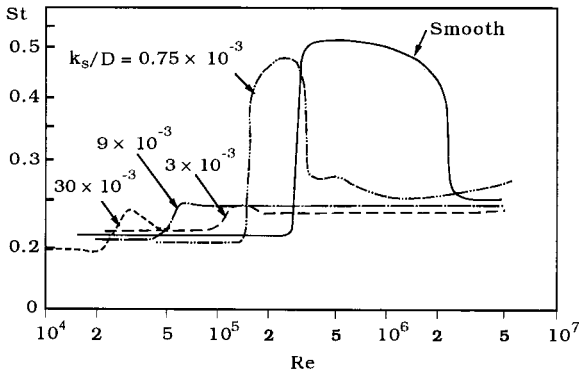


Figure 1.12 Effect of surface roughness on vortex-shedding frequency. Strouhal number against Reynolds number. Circular cylinder. Achenbach and Heinecke (1981).

Fig. 1.12 illustrates the effect of the relative roughness on the Strouhal number where the experimentally obtained St values for various values of k_s/D are plotted against Re (Achenbach and Heinecke, 1981). Clearly, the effect is significant. From the figure, it is apparent that, for rough cylinders with $k_s/D > 3 \times 10^{-3}$, the critical (the lower transition), the supercritical and the upper transition flow regimes merge into one narrow region in the $St-Re$ plane, and the flow regime switches directly to transcritical over this narrow Re range, and this occurs at very low values of Re number. (The figure indicates for example that, at $Re \approx 0.3 \times 10^5$ for $k_s/D = 30 \times 10^{-3}$ and at $Re \approx 1.5 \times 10^5$ for $k_s/D = 3 \times 10^{-3}$). This result is in fact anticipated, as it is well known that transition to turbulence occurs much earlier (i.e., at much smaller values of Reynolds number) over rough walls.

Example 1.1: Nikuradse's equivalent sand roughness

In practice there exists an extremely wide variety of surface roughnesses, from small protrusions existing in the texture of the surface itself to extremely large roughnesses in the form of marine growth such as mussels and acorn barnacles, etc..

Therefore, normally it is not an easy task to relate the roughness of the surface to some typical scale of the roughness elements, partly because the elements are quite unevenly distributed. (On a loose sand bed, for example, the roughness is measured to be 2-3 times the grain diameter). To tackle this problem, the concept "Nikuradse's equivalent sand roughness" has been introduced. The idea is to relate any kind of roughness to the Nikuradse roughness so that comparison can be made on the same basis. Very systematic and careful measurements on rough pipes were carried out by Nikuradse (1933), who used circular pipes. Sand with known grain size was glued on the pipe wall inside the pipe. By measuring the flow resistance and velocity profiles, Nikuradse obtained the following velocity distribution law

$$\frac{u}{U_f} = 5.75 \log_{10} \frac{y}{k_s} + 8.5 \quad (1.6)$$

which can be put in the following form

$$\frac{u}{U_f} = \frac{1}{\kappa} \ln \frac{30y}{k_s} \quad (1.7)$$

in which u is the streamwise velocity, U_f is the wall shear-stress velocity, κ is the Karman constant (≈ 0.4), y is the distance from the wall and k_s is the height of the sand roughness that Nikuradse used in his experiments (a detailed account of

the subject is given by Schlichting (1979)). To judge about the roughness of a particular surface, the usual practice is first to measure the velocity distribution above the surface in consideration and then, based on this measured velocity distribution $u(y)$, to determine k_s , the Nikuradse's equivalent sand roughness of the surface, from Eq. 1.7.

Effect of cross-sectional shape

Fig. 1.13 shows the Strouhal-number data compiled by Blevins (1977) for various non-circular cross sections, while Fig. 1.14 presents the Strouhal numbers for a variety of profile shapes compiled by ASCE Task Committee (1961). Modi, Wiland, Dikshit and Yokomizo (1992) give a detailed account of flow and vortex shedding around elliptic cross-section cylinders.

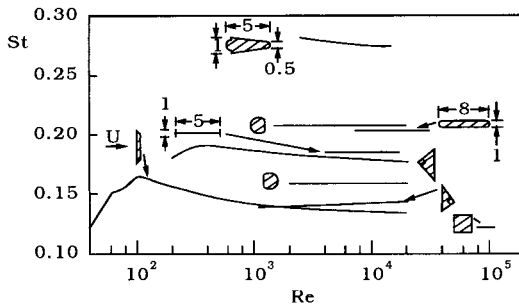


Figure 1.13 Effect of cross-sectional shape on vortex-shedding frequency. Strouhal number against Reynolds number. Blevins (1977).

As far as the large Reynolds numbers are concerned ($Re \gtrsim 10^5$), the vortex formation process is relatively uninfluenced by the Reynolds number for the cross sections with fixed separation points such as rectangular cylinders. So, the Strouhal number may not undergo large changes with increasing Re for such cross-sectional shapes, in contrast to what occurs in the case of circular cylinders.

Effect of incoming turbulence

Quite often, the approach flow is turbulent. For example, a cylinder placed on the sea bottom would feel the approach-flow turbulence which is generated within the bottom boundary layer. The turbulence in the approach flow is also an influencing factor with regard to the vortex shedding. The effect of turbulence

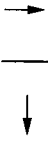
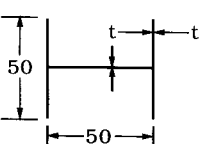

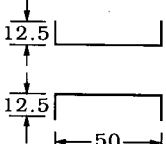
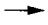
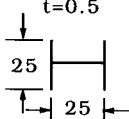

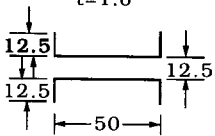

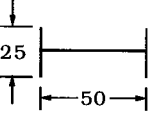

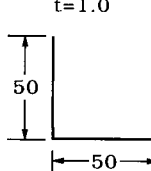



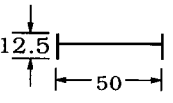

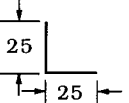

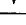
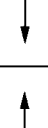
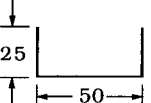
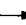
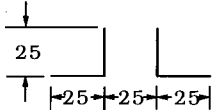

Flow	Profile Dimensions (mm)	Value of St	Flow	Profile Dimensions (mm)	Value of St
		0.120			0.147
		0.137			
		0.120			0.150
		0.144			0.145
					0.142
					0.147
		0.145			0.131
					0.134
					0.137
		0.140			0.121
					0.143
		0.153			

Figure 1.14 Effect of cross-sectional shape on Strouhal number. Strouhal numbers for profile shapes. ASCE Task Committee (1961).

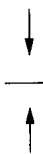
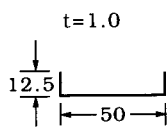

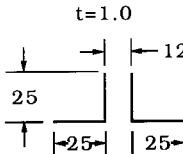
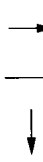
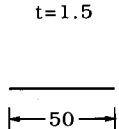
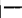
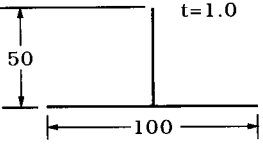

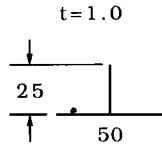
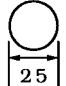
Flow	Profile Dimensions (mm)	Value of St	Flow	Profile Dimensions (mm)	Value of St
		0.145			0.135
		0.168			
		0.156			0.160
		0.145			
Cylinder $11800 < Re < 19100$		0.200			0.114
					0.145

Figure 1.14 (continued.)

on the vortex shedding has been studied by various authors, for example by Cheung and Melbourne (1983), Kwok (1986) and Norberg and Sundén (1987) among others. Fig. 1.15 presents the Strouhal number data obtained by Cheung and Melbourne for various levels of turbulence in their experimental tunnel. Here, I_u is the turbulence intensity defined by

$$I_u = \frac{\sqrt{u'^2}}{\bar{u}} \tag{1.8}$$

in which $\sqrt{u'^2}$ is the root-mean-square value of the velocity fluctuations and \bar{u} is the mean value of the velocity.

The variation of St with the Reynolds number changes considerably with the level of turbulence in the approach flow. The effect of turbulence is rather similar to that of cylinder roughness. The critical, the supercritical, and the upper transition flow regimes seem to merge into one transitional region.

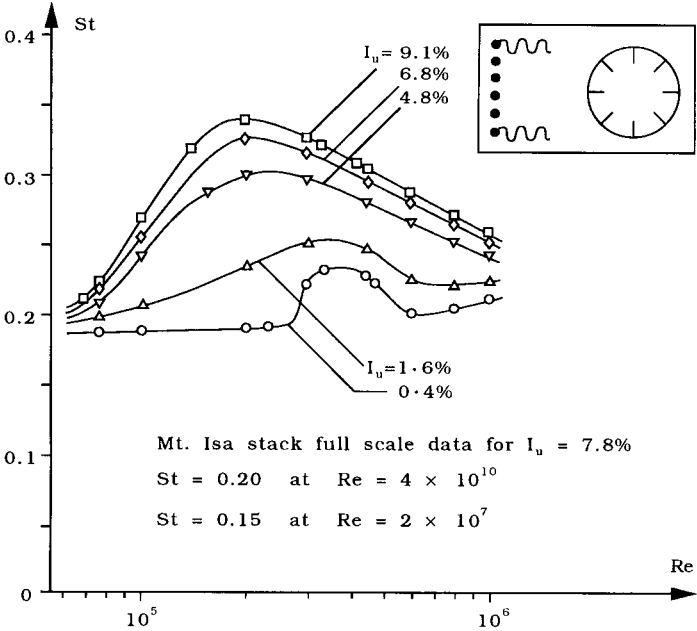


Figure 1.15 Effect of turbulence in the approach flow on vortex-shedding frequency. Strouhal numbers as a function of Reynolds number for different turbulence intensities. I_u is the level of turbulence (Eq. 1.8). Cheung and Melbourne (1983).

It appears from the figure that the lower end of this transition range shifts towards the smaller and smaller Reynolds numbers with the increased level of turbulence. This is obviously due to the earlier transition to turbulence in the cylinder boundary layer with increasing incoming turbulence intensity.

Effect of shear in the incoming flow

The shear in the approach flow is also an influencing factor in the vortex shedding process. The shear could be present in the approach flow in two ways: it could be present in the spanwise direction along the length of the cylinder (Fig. 1.16a), or in the cross-flow direction (Fig. 1.16b). The characteristics of shear flow around bluff bodies including the non-circular cross-sections have been reviewed by Griffin (1985a and b). In the case when the shear is present in the spanwise direction (Fig. 1.16a), the vortex shedding takes place in spanwise cells, with a

frequency constant over each cell. Fig. 1.17 clearly shows this; it is seen that the shedding occurs in four cells, each with a different frequency. When the Strouhal number is based on the local velocity (the dashed lines in the figure), the data are grouped around the Strouhal number of about 0.25.

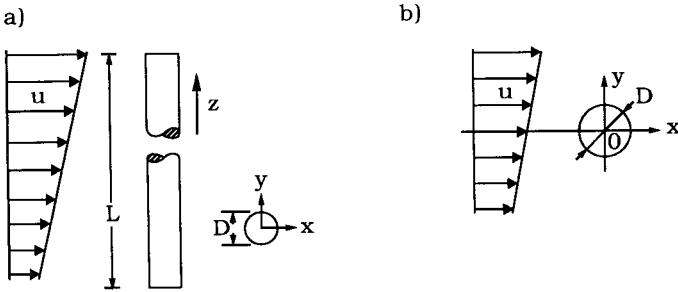


Figure 1.16 Two kinds of shear in the approach flow. a: Shear is in the spanwise direction. b: Shear is in the cross-flow direction.

Regarding the length of cellular structures, research shows that the length of cells is correlated with the degree of the shear. The general trend is that the cell length decreases with increasing shear (Griffin, 1985a).

When the shear takes place in the cross-stream direction (the conditions in the spanwise direction being uniform), the shedding is only slightly influenced for small and moderate values of the shear steepness s which is defined by

$$s = \frac{D}{U_c} \frac{du}{dy} \tag{1.9}$$

For large values of s , however, the shedding is influenced somewhat substantially (Kiya, Tamura and Arie, 1980). Fig. 1.18 shows the Strouhal number plotted against the Reynolds number for three different values of s . As is seen for $s = 0.2$, the Strouhal number is increased substantially relative to the uniform-flow case ($s = 0$).

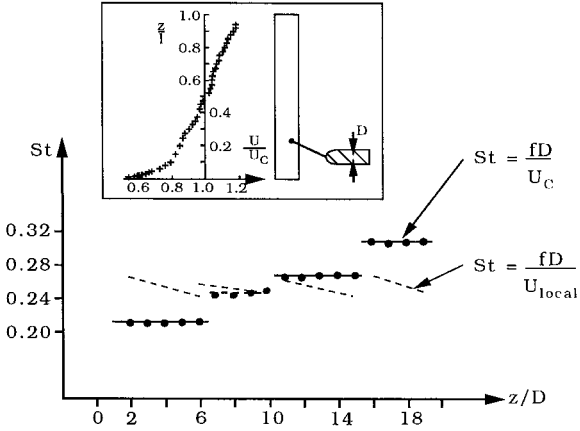


Figure 1.17 Effect of shear in the approach flow on vortex-shedding frequency. Shear in the spanwise direction. Circles: Strouhal number based on the centre-line velocity U_c . Dashed lines: Strouhal number based on the local velocity, U_{local} . $Re = 2.8 \times 10^4$. The shear steepness: $s = 0.025$. Maull and Young (1973).

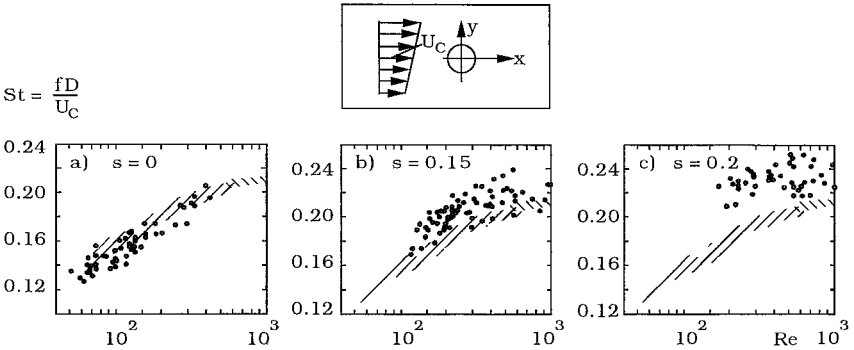


Figure 1.18 Effect of shear in the approach flow frequency. Shear in cross-flow direction. The Strouhal number against the Reynolds number for three different values of the shear steepness s . Hatched band: Uniform-flow results. Circles: Shear-flow results. Kiya et al. (1980).

Effect of wall proximity

This topic is of direct relevance with regard to pipelines. When a pipeline is placed on an erodible sea bed, scour may occur below the pipe due to flow action. This may lead to suspended spans of the pipeline where the pipe is suspended above the bed with a small gap, usually in the range from $O(0.1D)$ to $O(1D)$. Therefore it is important to know what kind of changes take place in the flow around and in the forces on such a pipe.

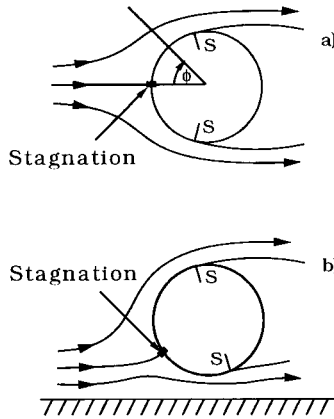


Figure 1.19 Flow around a) a free cylinder, b) a near-wall cylinder. S = separation points.

When a cylinder is placed near a wall, a number of changes occur in the flow around the cylinder. These changes are summarized as follows:

1) Vortex shedding is suppressed for the gap-ratio values smaller than about $e/D = 0.3$, as will be seen later in the section. Here, e is the gap between the cylinder and the wall.

2) The stagnation point moves to a lower angular position as sketched in Fig. 1.19. This can be seen clearly from the pressure measurements of Fig. 2.20a and Fig. 2.20b where the mean pressure distributions around the cylinder are given for three different values of the gap ratio. While the stagnation point is located at about $\phi = 0^\circ$ when $e/D = 1$, it moves to the angular position of about $\phi = -40^\circ$ when the gap ratio is reduced to $e/D = 0.1$.

3) Also, the angular position of the separation points changes. The separation point at the free-stream side of the cylinder moves upstream and that at the wall side moves downstream, as shown in the sketch given in Fig. 1.19. The

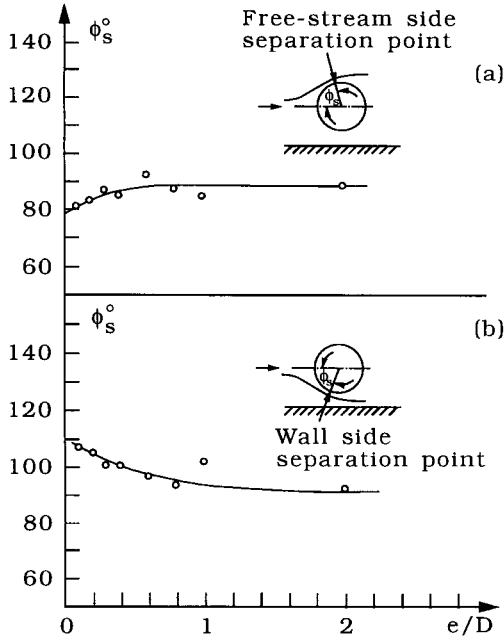


Figure 1.20 Angle of separation as a function of the gap ratio. (a): At the free-stream side of the cylinder and (b): At the wall side of the cylinder. $Re = 6 \times 10^3$. Jensen and Sumer (1986).

separation angle measured for a cylinder with $Re = 6 \times 10^3$ is shown in Fig. 1.20; the figure indicates that for example for $e/D = 0.1$ the separation angle at the free-stream side is $\phi \cong 80^\circ$, while it is $\phi \cong -110^\circ$ at the wall side for the same gap ratio.

4) Finally, the suction is larger on the free-stream side of the cylinder than on the wall-side of the cylinder, as is clearly seen in Fig. 2.20b and c. When the cylinder is placed away from the wall, however (Fig. 2.20a) this effect disappears and the symmetry is restored.

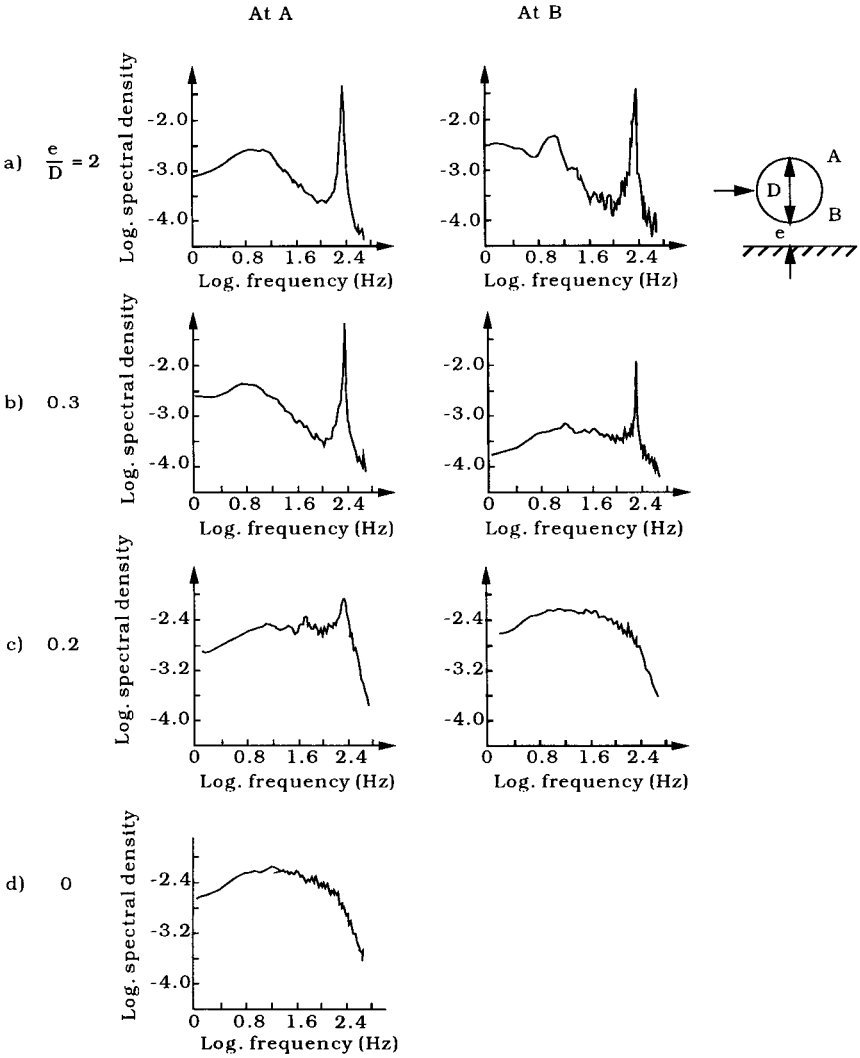


Figure 1.21 Effect of wall proximity on vortex shedding. Power spectra of the hot-wire signal received from the wake. Bearman and Zdravkovich (1978).

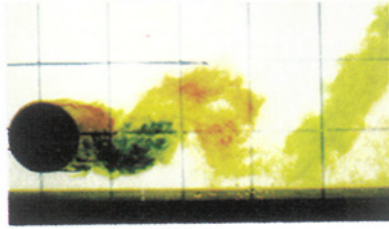
Vortex shedding may be suppressed for a cylinder which is placed close to a wall. Fig. 1.21 presents power spectra of the hot-wire signals received from both sides of the wake of a cylinder placed at different distances from a wall (Bearman and Zdravkovich, 1978). As is clearly seen, regular vortex shedding, identified by the sharply defined, dominant peaks in the power spectra, persists only for values of the gap-to-diameter ratio e/D down to about 0.3. This result, recognized first by Bearman and Zdravkovich, was later confirmed by the measurements of Grass, Raven, Stuart and Bray (1984). The photographs shown in Fig. 1.22 demonstrate the suppression of vortex shedding for gap ratios e/D below 0.3.

The suppression of vortex shedding is linked with the asymmetry in the development of the vortices on the two sides of the cylinder. The free-stream-side vortex grows larger and stronger than the wall-side vortex. Therefore the interaction of the two vortices is largely inhibited (or, for small e/D , totally inhibited), resulting in partial or complete suppression of the regular vortex shedding.

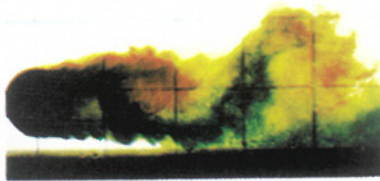
Regarding the effect of wall proximity on the vortex-shedding frequency for the range of e/D where the vortex shedding exists, measurements show that the shedding frequency tends to increase (yet slightly) with decreasing gap ratio. In Fig. 1.23 are plotted the results of two studies, namely Grass et al. (1984) and Raven, Stuart, Bray and Littlejohns (1985). Grass et al.'s experiments were done in a laboratory channel with both smooth and rough beds. The surface of the test cylinder was smooth. Their results collapse onto a common curve when plotted in the normalized form presented in the figure where St_0 is the Strouhal number for a wall-free cylinder. The data points of Raven et al.'s study, on the other hand, were obtained in an experimental program conducted in the Severn Estuary (UK) where a full-scale pipeline (50.8 cm in diameter with a surface roughness of $k/D = 8.5 \times 10^{-3}$) was used. In both studies, St is defined by the velocity at the top of the cylinder. There are other data available such as Bearman and Zdravkovich (1978) and Angrilli, Bergamaschi and Cossalter (1982). While Bearman and Zdravkovich's measurements indicate that the shedding frequency practically does not change over the range $0.3 \leq e/D \leq 3$, Angrilli et al.'s measurements show that there is a systematic (yet, slight) increase in the shedding frequency with decreasing gap ratio in their measurement range $0.5 \leq e/D \leq 6$ (they report a 10% increase in the shedding frequency at $e/D = 0.5$).

It is apparent from the existing data that the vortex-shedding frequency is insensitive to the gap ratio, although there seems to be a tendency that it increases slightly with decreasing gap ratio. This slight increase in the Strouhal frequency may be attributed to the fact that the presence of the wall causes the wall-side vortex to be formed closer to the free-stream-side vortex. As a result of this, the two vortices interact at a faster rate, leading to a higher St frequency.

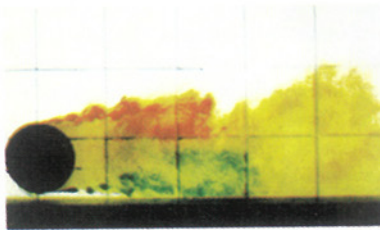
a) $\frac{e}{D} = 0.4$



b) $\frac{e}{D} = 0.3$



c) $\frac{e}{D} = 0.2$



d) $\frac{e}{D} = 0.05$

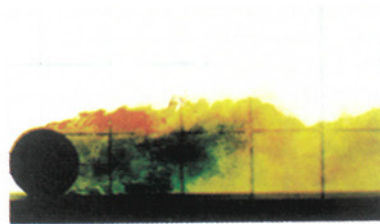


Figure 1.22 Effect of wall proximity on vortex shedding. Flow in the wake of a near-wall cylinder. Shedding is apparent for $e/D = 0.4$ and 0.3 but suppressed for $e/D = 0.2$ and 0.05 . $Re_e = 7 \times 10^3$.

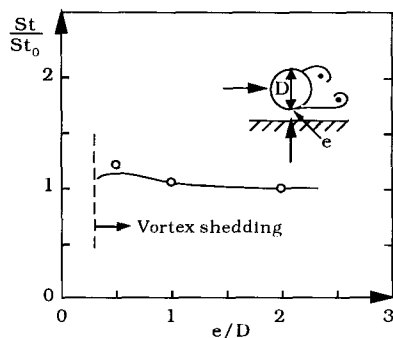


Figure 1.23 Effect of wall proximity on vortex shedding frequency. Normalized Strouhal number as a function of gap ratio. St_0 is the Strouhal number for wall-free cylinder. Circles: Raven et al. (1985). Solid curve: Grass et al. (1984).

Jensen, Sumer, Jensen and Fredsøe (1990) investigated the flow around a pipeline (placed initially on a flat bed) at five characteristic stages of the scour process which take place underneath the pipeline. Each stage was characterized in the experiments by a special, frozen scoured bed profile, which was an exact copy of the measured bed profile of an actual scour test. The investigated scour profiles and the corresponding mean flow field are shown in Fig. 1.24. It was observed that no vortex shedding occurred for the first two stages, namely stages I and II, while vortex shedding did occur for stages III - V. Fig. 1.25 depicts the shedding frequency corresponding to the different stages.

The variation of the Strouhal number, which goes from as high a value as 0.36 for Stage III to an equilibrium value of 0.17 in Stage V, can be explained by the geometry of the downstream scour profile as follows.

For profiles III and IV, the steep slope of the upstream part of the dune behind the cylinder forces the shear layer originating from the lower edge of the cylinder to bend upwards, thus causing the associated lower vortex to interact with the upper one prematurely, leading to a premature vortex shedding. The result of this is a higher vortex shedding frequency and a very narrow formation region. The flow visualization study carried out in the same experiments (Jensen et al., 1990) confirmed the existence of this narrow region.

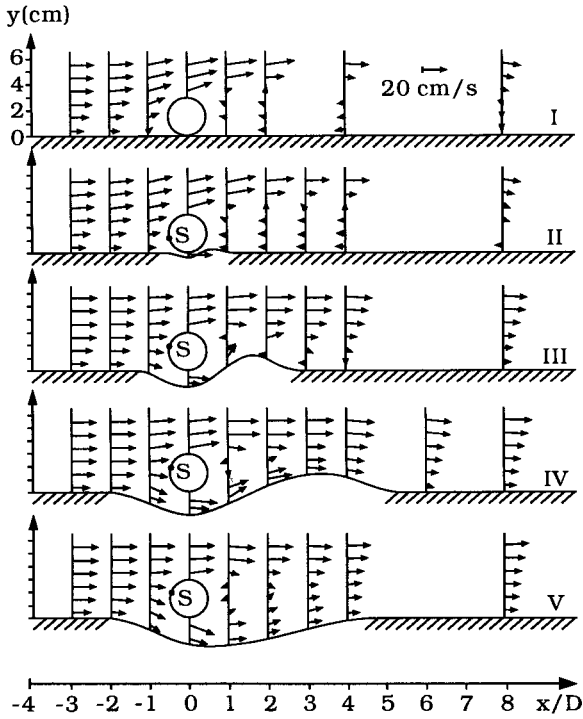


Figure 1.24 Vector plot of the mean velocities, S = the approximate position of the stagnation point. Jensen et al. (1990).

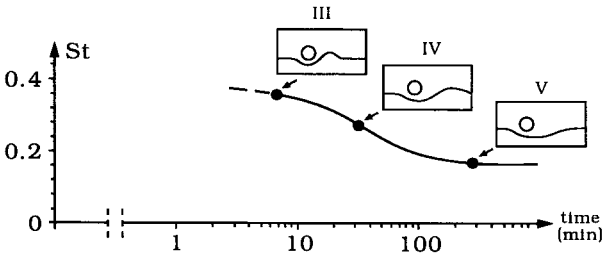


Figure 1.25 Time development of Strouhal number during the scour process below a pipeline. Jensen et al. (1990).

1.2.2 Correlation length

As has been mentioned in Section 1.1, vortex shedding in the turbulent wake regime (i.e. $Re > 200$) occurs in cells along the length of the cylinder.

These spanwise cell structures are visualized in Fig. 1.26 which shows the time evolution of the shedding process in plan view.

The cells are quite clear from the photographs in Fig. 1.26. Shedding does not occur uniformly along the length of the cylinder, but rather in cells (designated by A, B and C in Fig. 1.26). It can also be recognized from the pictures in Fig. 1.26 that the cells along the length of the cylinder are out of phase. Consequently, the maximum resultant force acting on the cylinder over its total length may be smaller than the force acting on the cylinder over the length of a single cell.

The average length of the cells may be termed the correlation length. The precise determination of the correlation length requires experimental determination of the spanwise variation of the correlation coefficient of some unsteady quantity related to vortex shedding, such as fluctuating surface pressure, or a fluctuating velocity just outside the shear layer at separation.

The correlation coefficient is defined by

$$R(z) = \frac{\overline{p'(\zeta) p'(\zeta + z)}}{\sqrt{\overline{p'^2(\zeta)}} \sqrt{\overline{p'^2(\zeta + z)}}} \quad (1.10)$$

in which ζ is the spanwise distance, z is the spanwise separation between two measurement points, and p' is the fluctuating part of the unsteady quantity in consideration. The overbar denotes the time averaging. The correlation length L , on the other hand, is defined by the integral

$$L = \int_0^\infty R(z) dz \quad (1.11)$$

Fig. 1.27 gives a typical example of the correlation coefficient obtained in a wind tunnel with a cylinder 7.6 cm in diameter and 91.4 cm in length with large streamlined end plates (Novak and Tanaka, 1977). The Reynolds number was 1.9×10^4 . The measured quantity was the surface pressure at an angle 60° to the main stream direction. The correlation length corresponding to the correlation coefficient, given in Fig. 1.27, on the other hand is found to be $L/D \cong 3$ from Eq. 1.11.

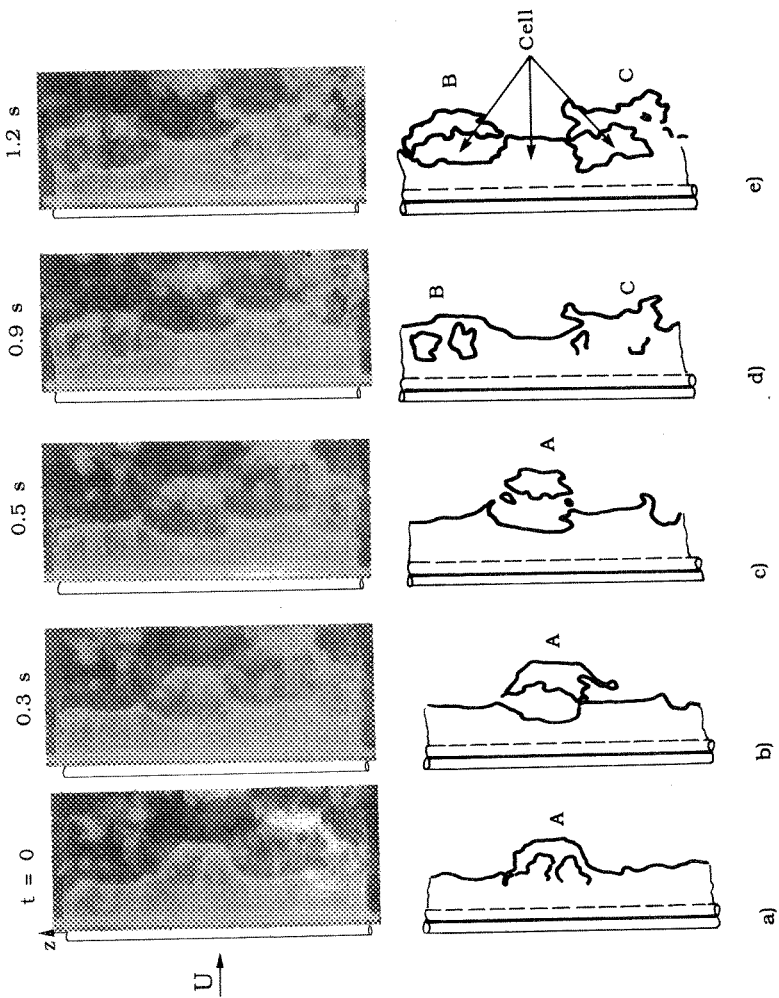


Figure 1.26 Photographs, illustrating the time evolution of spanwise cell structure. Cylinder smooth. $Re = 6 \times 10^3$.

For a smooth cylinder, the correlation length changes with the Reynolds number. Table 1.1 presents the correlation-length data compiled by King (1977).

Table 1.1 Correlation lengths and Reynolds numbers of smooth cylinders.

Reynolds number	Correlation length	Source
$40 < Re < 150$	$(15-20)D$	Gerlach and Dodge (1970)
$150 < Re < 10^5$	$(2-3)D$	Gerlach and Dodge (1970)
$1.1 \times 10^4 < Re < 4.5 \times 10^4$	$(3-6)D$	El-Baroudi (1960)
$\geq 10^5$	$0.5D$	Gerlach and Dodge (1970)
2×10^5	$1.56D$	Humphreys (1960)

The table shows that the correlation length is $(15-20)D$ for $40 < Re < 150$ but experiences a sudden drop to $(2-3)D$ at $Re = 150$. The latter Re number is quite close to the Reynolds number (see Fig. 1.1d), at which the laminar vortex shedding regime disappears. Regarding the finite (although large) values of the correlation length in the range $40 < Re < 150$, the correlation length in this flow regime should theoretically be infinite, since the vortex regime in this range is actually two-dimensional. However, purely two-dimensional shedding cannot be achieved in practice due to the existing end conditions. A slight divergence from the purely two-dimensional shedding, in the form of the so-called oblique shedding (see for example Williamson, 1989), may result in finite correlation lengths.

Other factors also affect the correlation. The correlation increases considerably when the cylinder is *oscillated* in the cross-flow direction. Fig. 1.28 presents the correlation coefficient data obtained by Novak and Tanaka (1977) for several values of the double-amplitude-diameter ratio $2A/D$ where A is the amplitude of cross-flow vibrations of the cylinder. The figure shows that the correlation coefficient increases tremendously with the amplitude of oscillations. Similar results were obtained by Toebes (1969) who measured the correlation coefficient of fluctuating velocity in the wake region near the cylinder. Fig. 1.29 presents the variation of the correlation length as a function of the amplitude-to-diameter ratio (curve a in Fig. 1.29). Clearly, the correlation length increases extensively with increasing the amplitude of oscillations.

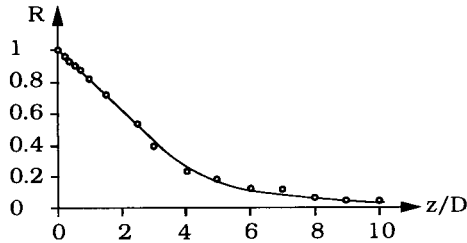


Figure 1.27 Correlation coefficient of surface pressure fluctuations as function of the spanwise separation distance z . Cylinder smooth. $Re = 1.9 \times 10^4$. Pressure transducers are located at 60° to the main stream direction. Novak and Tanaka (1977).

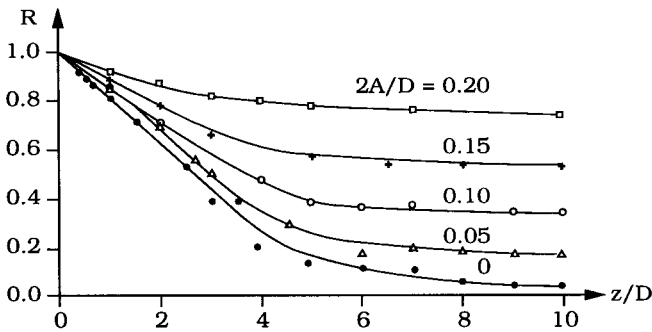


Figure 1.28 Effect of cross-flow vibration of cylinder on correlation coefficient of surface pressure fluctuations. Cylinder smooth. $Re = 1.9 \times 10^4$. Pressure transducers are located at 60° to the main stream direction. A is the amplitude of the cross-flow vibrations of cylinder. Novak and Tanaka (1977).

Turbulence in the approaching flow is also a significant factor for the correlation length, as is seen from Fig. 1.29. The turbulence in the tests presented in this figure was generated by a coarse grid in the experimental tunnel used in Novak and Tanaka's (1977) study. The figure indicates that the presence of turbulence

in the approaching flow generally reduces the correlation length. It is interesting to note that with $2A/D = 0.2$, while the correlation length increases from about 3 diameters to 43 diameters for a turbulence-free, smooth flow, the increase is not so dramatic when some turbulence is introduced into the flow; the correlation length increases to only about 10 diameters in this latter situation.

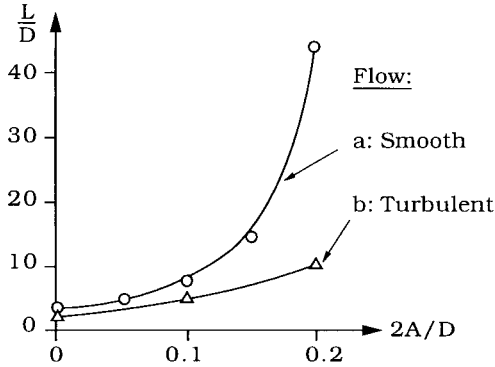


Figure 1.29 Correlation length. Cylinder smooth. $Re = 1.9 \times 10^4$. Pressure transducers are located at 60° to the main stream direction. A is the amplitude of cross-flow vibrations of the cylinder. Turbulence in the tunnel was generated by a coarse grid, and its intensity, $I_u = 11\%$. Novak and Tanaka (1977).

The subject has been most recently studied by Szepessy and Bearman (1992). These authors studied the effect of the aspect ratio (namely the cylinder length-to-diameter ratio) on vortex shedding by using moveable end plates. They found that the vortex-induced lift showed a maximum for an aspect ratio of 1, where the lift could be almost twice the value for very large aspect ratios. This increase of the lift amplitude was found to be accompanied by enhanced spanwise correlation of the flow.

Finally, it may be noted that Ribeiro (1992) gives a comprehensive review of the literature on oscillating lift on circular cylinders in cross-flow.

REFERENCES

- Achenbach, E. and Heinecke E. (1981): On vortex shedding from smooth and rough cylinders in the range of Reynolds numbers 6×10^3 to 5×10^6 . *J. Fluid Mech.*, 109:239-251.
- Angrilli, F., Bergamaschi, S. and Cossalter, V. (1982): Investigation of wall-induced modifications to vortex shedding from a circular cylinder. *Trans. of the ASME, J. Fluids Engrg.*, 104:518-522.
- ASCE Task Committee on Wind Forces (1961): Wind forces on structures. *Trans. ASCE*, 126:1124-1198.
- Batchelor, G.K. (1967): *An Introduction to Fluid Dynamics*. Cambridge University Press.
- Bearman, P.W. and Zdravkovich, M.M. (1978): Flow around a circular cylinder near a plane boundary. *J. Fluid Mech.*, 89(1):33-48.
- Blevins, R.D. (1977): *Flow-induced Vibrations*. Van Nostrand.
- Bloor, M.S. (1964): The transition to turbulence in the wake of a circular cylinder. *J. Fluid Mech.*, 19:290-304.
- Cheung, J.C.K. and Melbourne, W.H. (1983): Turbulence effects on some aerodynamic parameters of a circular cylinder at supercritical Reynolds numbers. *J. of Wind Engineering and Industrial Aerodynamics*, 14:399-410.
- El-Baroudi, M.Y. (1960): *Measurement of Two-Point Correlations of Velocity near a Circular Cylinder Shedding a Karman Vortex Street*. University of Toronto, UTIAS, TN31.
- Farell, C. (1981): Flow around fixed circular cylinders: Fluctuating loads. *Proc. of ASCE, Engineering Mech. Division*, 107:EM3:565-588. Also see the closure of the paper. *Journal of Engineering Mechanics, ASCE*, 109:1153-1156, 1983.
- Gerlach, C.R. and Dodge, F.T. (1970): An engineering approach to tube flow-induced vibrations. *Proc. Conf. on Flow-Induced Vibrations in Reactor System Components*, Argonne National Laboratory, pp. 205-225.
- Gerrard, J.H. (1966): The mechanics of the formation region of vortices behind bluff bodies. *J. Fluid Mech.*, 25:401-413.

- Gerrard, J.H. (1978): The wakes of cylindrical bluff bodies at low Reynolds number. *Phil. Transactions of the Royal Soc. London, Series A*, 288(A1354):351-382.
- Grass, A.J., Raven, P.W.J., Stuart, R.J. and Bray, J.A. (1984): The influence of boundary layer velocity gradients and bed proximity on vortex shedding from free spanning pipelines. *Trans. ASME, J. of Energy Res. Technology*, 106:70-78.
- Griffin, O.M. (1985a): Vortex shedding from bluff bodies in a shear flow: A Review. *Trans. ASME, J. Fluids Eng.*, 107:298-306.
- Griffin, O.M. (1985b): The effect of current shear on vortex shedding. *Proc. Int. Symp. on Separated Flow Around Marine Structures. The Norwegian Inst. of Technology, Trondheim, Norway, June 26-28, 1985*, pp. 91-110.
- Homann, F. (1936): Einfluss grosser Zähigkeit bei Strömung um Zylinder. *Forschung auf dem Gebiete des Ingenieurwesen*, 7(1):1-10.
- Humphreys, J.S. (1960): On a circular cylinder in a steady wind at transition Reynolds numbers. *J. Fluid Mech.*, 9:603-612.
- Jensen, B.L. and Sumer, B.M. (1986): Boundary layer over a cylinder placed near a wall. *Progress Report No. 64, Inst. of Hydrodynamics and Hydraulic Engineering, ISVA, Techn. Univ. Denmark*, pp. 31-39.
- Jensen, B.L., Sumer, B.M., Jensen, H.R. and Fredsøe, J. (1990): Flow around and forces on a pipeline near a scoured bed in steady current. *Trans. of the ASME, J. of Offshore Mech. and Arctic Engrg.*, 112:206-213.
- King, R. (1977): A review of vortex shedding research and its application. *Ocean Engineering*, 4:141-171.
- Kiya, M., Tamura, H. and Arie, M. (1980): Vortex shedding from a circular cylinder in moderate-Reynolds-number shear flow. *J. Fluid Mech.*, 141:721-735.
- Kwok, K.C.S. (1986): Turbulence effect on flow around circular cylinder. *J. Engineering Mechanics, ASCE*, 112(11):1181-1197.
- Maull, D.J. and Young, R.A. (1973): Vortex shedding from bluff bodies in a shear flow. *J. Fluid Mech.*, 60:401-409.
- Modi, V.J., Wiland, E., Dikshit, A.K. and Yokomizo, T. (1992): On the fluid dynamics of elliptic cylinders. *Proc. 2nd Int. Offshore and Polar Engrg. Conf., San Francisco, CA, 14-19 June 1992*, III:595-614.

- Nikuradse, J. (1933): Strömungsgesetze in rauhen Rohren. *Forsch. Arb.Ing.-Wes.* No. 361.
- Norberg, C. and Sundén, B. (1987): Turbulence and Reynolds number effects on the flow and fluid forces on a single cylinder in cross flow. *Jour. Fluids and Structures*, 1:337-357.
- Novak, M. and Tanaka, H. (1977): Pressure correlations on a vibrating cylinder. *Proc. 4th Int. Conf. on Wind Effects on Buildings and Structures*, Heathrow, U.K., Ed. by K.J. Eaton. Cambridge Univ. Press, pp. 227-232.
- Raven, P.W.J., Stuart, R.J., Bray, J.A. and Littlejohns, P.S. (1985): Full-scale dynamic testing of submarine pipeline spans. 17th Annual Offshore Technology Conference, Houston, Texas, May 6-9., paper No. 5005, 3:395-404.
- Ribeiro, J.L.D. (1992): Fluctuating lift and its spanwise correlation on a circular cylinder in a smooth and in a turbulent flow: a critical review. *Jour. of Wind Engrg. and Indust. Aerodynamics*, 40:179-198.
- Roshko, A. (1961): Experiments on the flow past a circular cylinder at very high Reynolds number. *J. Fluid Mech.*, 10:345-356.
- Schewe, G. (1983): On the force fluctuations acting on a circular cylinder in cross-flow from subcritical up to transcritical Reynolds numbers. *J. Fluid Mech.*, 133:265-285.
- Schlichting, G. (1979): *Boundary Layer Theory*. 7.ed. McGraw-Hill Book Company.
- Szepessy, S. and Bearman, P.W. (1992): Aspect ratio and end plate effects on vortex shedding from a circular cylinder. *J. Fluid Mech.*, 234:191-217.
- Toebes, G.H. (1969): The unsteady flow and wake near an oscillating cylinder. *Trans. ASME J. Basic Eng.*, 91:493-502.
- Williamson, C.H.K. (1988): The existence of two stages in the transition to three-dimensionality of a cylinder wake. *Phys. Fluids*, 31(11):3165-3168.
- Williamson, C.H.K. (1989): Oblique and parallel modes of vortex shedding in the wake of a circular cylinder at low Reynolds number. *J. Fluid Mech.*, 206:579-627.